GIScience Integrated with Computer Vision for the Interpretation and Analysis of Old Paintings

Motti Zohar[1][a], Ilan Shimshoni[2][b] and Fadi Khateb[2]
[1]*Department of Geography and Environmental Studies, University of Haifa, Israel*
[2]*Department of Information Systems, University of Haifa, Israel*

Keywords: GIScience, Computer Vision, Geo-referencing, Cartography, Jerusalem.

Abstract: Photographs of Ottoman Palestine are available only from the 2nd half of the 19th century onward. Thus, in order to reconstruct the landscape at the time one should rely on other visual sources such as old paintings. To do so, their accuracy and completeness must be addressed first. In this paper we analyse a painting from 1823 by the British Sir Frederick Henniker that drew the Old City of Jerusalem when standing somewhere on the Mount of Olives. We use GIScience techniques with computer vision capabilities to resolve the exact location where the artist stood as well as verifying errors and completeness of the painting. Preliminary results demonstrate that the location of the artist when drawing the painting was on top of Mount of Olives (close to present-day 7 arches hotel) rather at the Cave of the Apostles as cited in the NLI librarian citation. Additionally, the accuracy of his work was verified by comparing the features he drew on the canvas to their actual location on a present-day photograph.

1 INTRODUCTION

In 1820 the British traveller, Sir Frederick Henniker (1793-1825), visited Ottoman Palestine (Ben-Arieh, 1997, p. 30). In his book from 1823 he presented a painting of the Old City of Jerusalem alleged to be drawn from the Cave of the Apostles located at the western slope of the Mount of Olives (Henniker, 1823). Henniker portrayed the Old City surrounded by the 16th century Ottoman walls along with other prominent structures and monuments, some are still standing till present-day (Fig. 1). Photography in Palestine was not available until the 2nd half of the 19th century (Nir, 1985). Thus, Henniker's painting as well as paintings of other artists (Röhricht, 1890) may serve as a meaningful resource for past landscape reconstructions in periods prior to the mid-19th century. However, relying on historical paintings must be done carefully whereas they might be inaccurate, incomplete and subjected to the artist's perception and conceptualization of reality.

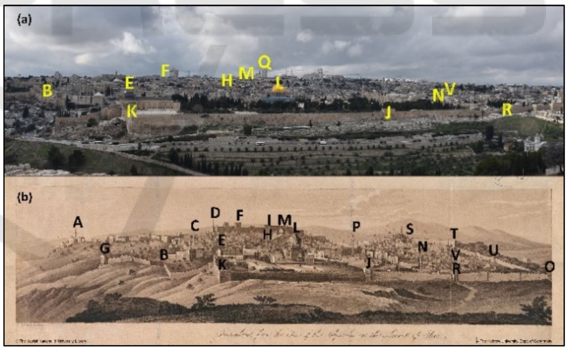

Figure 1: (a) The Old City of Jerusalem photographed from the Mount of Olives (photographing: Motti Zohar, January 2020). Prominent features are noted in black on the photograph e.g., E (Al Aqsa mosque), L (Dome of the Rock), M (Church of the Holy Sepulchre) and Q (the Custodia Terra Sancta); (b) The painting of Henniker from 1823. See the complete list of notations in Table 1 in the Appendix.

[a] https://orcid.org/0000-0002-6567-7296
[b] https://orcid.org/0000-0002-5276-0242

Zohar, M., Shimshoni, I. and Khateb, F.
GIScience Integrated with Computer Vision for the Interpretation and Analysis of Old Paintings.
DOI: 10.5220/0009464902330239
In *Proceedings of the 6th International Conference on Geographical Information Systems Theory, Applications and Management (GISTAM 2020)*, pages 233-239
ISBN: 978-989-758-425-1

2 GIScience AND COMPUTER VISION

The rapid development of GIS (Geographic Information Systems) and GIScience (Geographic Information Science) during the last few decades have revolutionized the way scientists manage and analyse spatial data (Goodchild, 2010). With quantitative and qualitative capabilities (Cope & Elwood, 2009; Y. Wang & Taylor, 2018) GIS serves a wide range of spatial applications (Sui, 2015) and forms a proper platform to verify spatial hypotheses. As far as cartography is concerned, GIScience enables spatial analyses (Levin, 2006; Schaffer et al., 2016; Zohar, 2019); the creation of deep maps as multimedia conveyors of places and their everyday lives (Bodenhamer et al., 2015); and the inspection of narratives using map stories (Antoniou et al., 2018; Mennis et al., 2013). In historical-based studies, GIScience is used in creating new forms of virtual knowledge (Gregory & Healy, 2007; Knowles, 2008); performing 2D and 3D landscape reconstructions (e.g., Davie & Frumin, 2007; Georgoula et al., 2013; Nakaya et al., 2010; Rubinowicz & Czyńska, 2015; Zohar, 2017); and resolving complex scenarios of past phenomena (e.g., Bender et al., 2005; Katz & Crouvi, 2007; Verhagen & Jeneson, 2012).

Like GIS, computer vision and especially machine learning based computer vision have undergone major advances over the last two decades enriching also the GIS capabilities and automating tedious processes such as feature extraction and digitization (e.g., Chen et al., 2018; Fanos et al., 2018; Garosi et al., 2019; Naghibi et al., 2016). Methods can therefore be applied and developed for addressing problems of interpretation of historical visual sources. These include methods for registration of photographs as an addition to geo-referencing maps (Aubry et al., 2014; Goshen & Shimshoni, 2008; Hartley & Zisserman, 2003). Once a given source has been aligned and registered, the use of machine learning may assist in extracting and aligning features such as roads and buildings (Duan et al., 2017; Uhl et al., 2017; J. Wang et al., 2015).

The goal of the study is to interpret the old painting of Henniker using GIScience approaches integrated with computation vision capabilities. In this short paper we attempt to address the following two questions: (1) What used to be the location of the artist when he drew the painting? (2) What are the errors made by the artist in comparison to actual view of Jerusalem? We hypothesize that computer vision capabilities may empower and semi-automate the GIScience approaches initiated so far in analysing old paintings during the processes of geo-referencing, digitization and errors verification. Accordingly, we present preliminary results of the implemented methodology aimed at addressing these problems of interpreting old paintings.

3 METHODOLOGY

3.1 The GIS Environment

We use the ESRI© ArcGIS Pro software as our base platform for the analysis and the Israel Transverse Mercator (ITM) (Mugnier, 2000) as the preferred Coordinate Reference System (CRS). For coding we use Python which can be run both internally within the ArcGIS Pro suit and by an external IDE (Integrated Development Environment). The geospatial data we have used as GIS layers for our analysis is (1) present-day orthophoto of Jerusalem with a resolution of 0.35 meter/pixel; (2) The mid-19th century Jerusalem map of Wilson (1865); and (3) Digital Elevation Model (DEM) of the Advanced Land Observation Satellite–Phased Array type L-band Synthetic Aperture Radar (ALOS-PALSAR) with a resolution of 12.5 meter/pixel (http://www.eorc.jaxa.jp/ALOS/en/about/palsar.htm) downloaded from https://vertex.daac.asf.alaska.edu/#

3.2 3D Features as Control Points

We have noted as control points 22 prominent features appearing in the painting of Henniker as well as in the map of Wilson and still exist till present-day (Figures 1, 2 and Table 1 in the Appendix). For each feature, we have extracted the parameters of longitude, latitude and absolute elevation (above sea level) using the DEM. Additionally, we have calculated the height above surface of each feature using measurements taken in field and also those made by Alud and Hillenbrand (2000). Given the orientation of the painting as looking from the Mount of Olives from east to west towards the Old City of Jerusalem (Fig. 1), a study area of nearly 1 square kilometre, elongated south to north, was delineated along the ridge of Mount of Olives (Fig 2) as a plausible area in which the artist might have stood while he was completing his work.

3.3 Line of Sight

We assume the artist was painting what he was able to observe. In other words, the 22 noted features were probably visible to him from the location of drawing. Accordingly, the delineated study area was gridded into cells of 0.25*0.25 meters, resulting in 158412 potential observation points along the Mount of Olives. Then, a visibility line of sight for each of the potential observation point was evaluated. That is, how many of the 22 noted features can be seen from each of the observation points. The visibility evaluation took into consideration a 6-8 m height of the surrounding Ottoman walls as sight obstacles and an offset of 2 meters above the surface as the observer height. The frequency of the visible features from the observation points that are within the delineated study area is presented in Figure 3. Accordingly, the area in which all 22 features are visible is portrayed in black while region with limited visibility are portrayed in purple. Not surprisingly, the visibility results are primarily dictated by height differences, although artificial structures such as buildings may also influence but were omitted from the analysis.

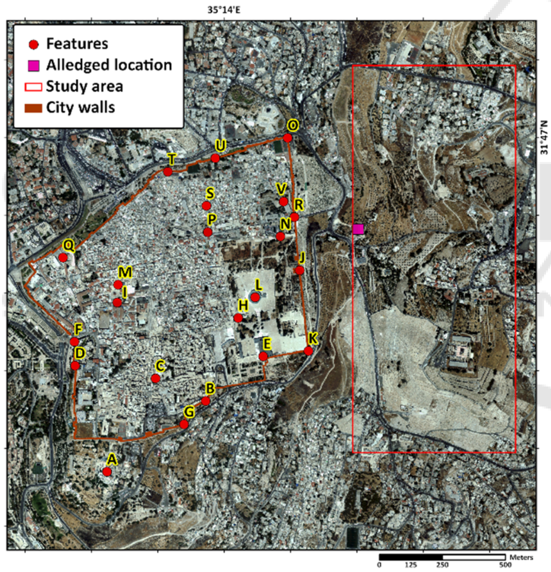

Figure 2: Aerial photography of present-day Old City of Jerusalem and the delineated study area on the Mount of Olives (outlined in red). The alleged location of the artist (Cave of the Apostles) as cited in the librarian record of the NLI (National Library of Israel) is presented a purple square.

3.4 Computer Vision Feature Matching

Assuming the painting is equivalent to a photograph, a robust RANSAC (Fischler & Bolles, 1981; Hartley & Zisserman, 2003) algorithm was implemented, which recovered the position, orientation, and parameters of the "camera" (the artist position). In theory it is impossible to separate the focal length of the camera (it's zoom) and the distance from the scene. Therefore, constraints on the artist's position were given in association with a given observation point. This is important for verifying the horizontal and vertical accuracy of the painting.

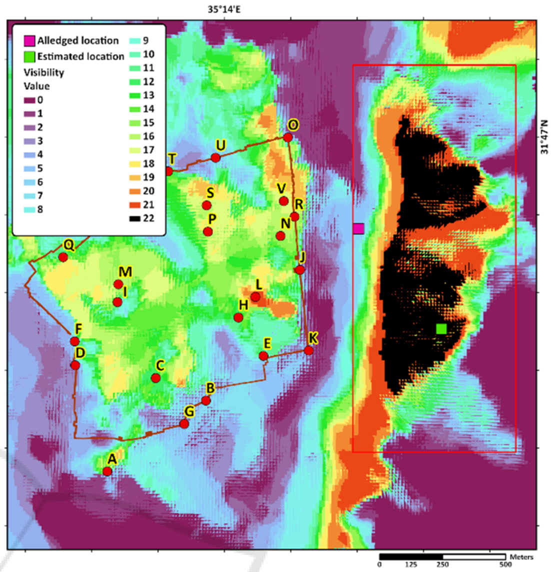

Figure 3: Visibility of the 22 noted features in and around the Old City of Jerusalem. The potential observation points where all features are visible are depicted in black.

4 PRELIMINARY RESULTS

4.1 The Location of the Artist

According to the NLI (National Library of Israel) citation, the alleged location where the artist stood when he drew the painting was at the Cave of the Apostles on the western slope of Mount of Olives (at elevation of 720 m above sea level) (Figure 2). Following the iteration of the RANSAC model on each of the potential observation points, it was found that the observation point with the highest score is on top of the mountain at coordinates 631574N, 223120E (at elevation of 794 m above sea level, close to present-day Seven Arches Hotel) (Figure 3). The elevation difference of 74 meters between the alleged and calculated locations explains why the Cave of the Apostles is not a reasonable location; had the artist stood at this position, he could have barely seen any of the features within the Old City. In other words, the relative height inferiority of the Cave of the Apostles in compare to the Old City and the surrounding

Ottoman walls, blocks the possibility to observe any structure located within the city. On the other hand, our calculated location (using the RANSAC model) confirms a clear line of sight from this observation point to each of the 22 features as demonstrated in Figure 1a that was photographed from the same location.

4.2 Errors Made by the Artist

Figure 4a presents the identification of the 22 features noted on the painting and the equivalent identification of the RANSAC model (green and red lines), which corresponds to the observation point with the highest suitability score (Figure 3). For comparison, we have implemented a RANSAC model on a present-day photograph (Figure 4b) taken from the same position. The results of the RANSAC models on both the painting and photograph are used for orientation and identifying notation errors (on the photograph) and errors made by the artist (in the painting).

Table 1 (see Appendix) presents the differences in pixels between the feature notations in compare to the notations achieved by the RANSAC model. The errors (in pixels) are listed in fields EH and EP for Henniker's painting and the photograph with average error values of 56 and 51 pixels, respectively. The errors distributions were then classified into quartiles and the those included in 4th quartile were inspected. Accordingly, the features with higher error values are T, U and of lesser extent G and O on Henniker's painting and F and R on the present-day photograph (Table 1 in the Appendix). The prominent high elevated feature Q (the Custodia Terra Sancta) on the present-day photograph was not detected on Henniker's' painting; perhaps it may explain an error of the artist when portraying a none-identified minaret at the northwestern corner of the Old City. The errors of features T, U and O are 195, 196 and 89 pixels, respectively. These features are located at the north of the city (on the right wing of the painting) imply that the artist may have overestimated lengths at the northern region which offsets his vision. Clearly the center of the city was more visible to the artist thus enabling better approximation of lengths from the location he was standing when drawing the painting (Figure 3). The slight errors of the RANSAC model on the present-day photograph may result from potential distortion of the focal lens and will be verified during the next stages of the study. Overall, the average error of the Henniker painting is slightly bigger than that of the photograph (56 pixels in comparison to 51 pixels) implying that the artist was quite accurate when drawing the scene and the included prominent features.

5 CONCLUSIONS

In this paper we present preliminary results of a methodology combining GIScience and computer vision capabilities to cope with the inaccuracy associated with historical visual sources such as old paintings. The methodology used is at its first stages and is being currently further developed. Yet, it enables already at this point to track the position of the artist when he drew the painting thus contradicting the alleged location to be at the Cave of the Apostles as cited in the painting's library record at the NLI. We have also managed to verify the accuracy of features on the painting's canvas, perhaps drew by the artist with less accuracy due to sharp offset from the location he was standing or in order to meet his subjective perception. Additionally, we were able to identify errors on the painting in compare to present-day photograph by comparing the two sets of results. Yet, to this point there are some vague identification in Henniker's painting which we could have not resolved by the RANSAC model such as the Custodia Terra Sancta location and the anonymous minaret at the north section of the Old City.

The potential contribution of establishing complete framework for analysing old paintings and illustrations is enormous for historical-based studies. In the next stages we will test additional paintings and attempt to spatially register the included features within a known Coordinate Reference System (CRS). We anticipate this process will re-project the features on the canvas of the painting back to the GIS framework. We will test our results with past and present-day photographs.

Figure 4: Noted features on Henniker's painting (a) and present-day photograph (b) The lines represent the RANSAC identification whereas green lines denote small-scale error detection while red lines stand for relatively large errors. For complete results see also Table 1 in the Appendix.

REFERENCES

Alud, S., & Hillenbrand, R. (2000). *Ottoman Jerusalem* (Vol. 1). London: Altajir World of Islam Trust.

Antoniou, V., Ragia, L., Nomikou, P., Bardouli, P., Lampridou, D., Ioannou, T., Kalisperakis, I., & Stentoumis, C. (2018). Creating a story map using geographic information systems to explore geomorphology and history of Methana peninsula. *ISPRS International Journal of Geo-Information, 7*(12), 484.

Aubry, M., Maturana, D., Efros, A. A., Russell, B. C., & Sivic, J. (2014). *Seeing 3d chairs: exemplar part-based 2d-3d alignment using a large dataset of cad models*.

Ben-Arieh, Y. (1997). *Painting the Holy Land in the Nineteenth Century*. Jerusalem: Yad Izhak Ben-Zvi Publications.

Bender, O., Boehmer, H. J., Jens, D., & Schumacher, K. P. (2005). Using GIS to analyse long-term cultural landscape change in Southern Germany. *Landscape and Urban Planning, 70*(1–2), 111-125. doi: 10.1016/j.landurbplan.2003.10.008.

Bodenhamer, D. J., Corrigan, J., & Harris, T. M. (2015). *Deep maps and spatial narratives*: Indiana University Press.

Chen, W., Li, H., Hou, E., Wang, S., Wang, G., Panahi, M., Li, T., Peng, T., Guo, C., & Niu, C. (2018). GIS-based groundwater potential analysis using novel ensemble weights-of-evidence with logistic regression and functional tree models. *Science of the Total Environment, 634*, 853-867.

Cope, M., & Elwood, S. (2009). *Qualitative GIS: a mixed methods approach*: Sage.

Davie, F. M., & Frumin, M. (2007). Late 18th century Russian Navy maps and the first 3D visualization of the walled city of Beirut. *e-Perimetron, 2*(2), 52-65.

Duan, W., Chiang, Y.-Y., Knoblock, C. A., Jain, V., Feldman, D., Uhl, J. H., & Leyk, S. (2017). *Automatic alignment of geographic features in contemporary vector data and historical maps*.

Fanos, A. M., Pradhan, B., Mansor, S., Yusoff, Z. M., & bin Abdullah, A. F. (2018). A hybrid model using machine learning methods and GIS for potential rockfall source identification from airborne laser scanning data. *Landslides, 15*(9), 1833-1850.

Fischler, M. A., & Bolles, R. C. (1981). Random sample consensus: a paradigm for model fitting with applications to image analysis and automated cartography. *Communications of the ACM, 24*(6), 381-395.

Garosi, Y., Sheklabadi, M., Conoscenti, C., Pourghasemi, H. R., & Van Oost, K. (2019). Assessing the performance of GIS-based machine learning models with different accuracy measures for determining susceptibility to gully erosion. *Science of the Total Environment, 664*, 1117-1132.

Georgoula, O., Stamnas, A., Patias, P., Georgiadis, C., & Fragkoulidou, V. (2013). Historical coastal urban landscapes digital documentation and temporal study with 2D/3D modeling functionality: The case of Thessaloniki, Greece. *Journal of Cultural Heritage, 14*(5), 396-402.

Goodchild, M. F. (2010). Twenty years of progress: GIScience in 2010. *Journal of spatial information science, 2010*(1), 3-20.

Goshen, L., & Shimshoni, I. (2008). Balanced exploration and exploitation model search for efficient epipolar geometry estimation. *IEEE Transactions on Pattern Analysis and Machine Intelligence, 30*(7), 1230-1242.

Gregory, I. N., & Healy, G. R. (2007). Historical GIS: structuring, mapping and analysing geographies of the past. *Progress in Human Geography, 31*(5), 638-653. doi: 10.1177/0309132507081495.

Hartley, R., & Zisserman, A. (2003). *Multiple view geometry in computer vision*: Cambridge university press.

Henniker, F. (Cartographer). (1823). Jerusalem from the Cave of the Apostles on the Mount of Olives. Drawn by F. Henniker. Engraved by G. Hunt.

Katz, O., & Crouvi, O. (2007). The geotechnical effects of long human habitation (2000 < years): Earthquake induced landslide hazard in the city of Zefat, northern Israel. *Engineering Geology, 95*(3-4), 57-78.

Knowles, A. K. (2008). *Placing History: How Maps, Spatial Data, and GIS are Changing Historical Scholarship*. Redlands, California: ESRI Press.

Levin, N. (2006). The Palestine exploration fund map (1871–1877) of the holy land as a tool for analyzing landscape changes: the coastal dunes of Israel as a case study. *The Cartographic Journal, 43*(1), 45-67. doi: 10.1179/000870406X93508.

Mennis, J., Mason, M. J., & Cao, Y. (2013). Qualitative GIS and the visualization of narrative activity space data. *International Journal of Geographical Information Science, 27*(2), 267-291.

Mugnier, C. J. (2000). Grids and datums: the state of Israel. *Photogrammetric Engineering & Remote Sensing, 66*(8), 915-917.

Naghibi, S. A., Pourghasemi, H. R., & Dixon, B. (2016). GIS-based groundwater potential mapping using boosted regression tree, classification and regression tree, and random forest machine learning models in Iran. *Environmental monitoring and assessment, 188*(1), 44.

Nakaya, T., Yano, K., Isoda, Y., Kawasumi, T., Takase, Y., Kirimura, T., Tsukamoto, A., Matsumoto, A., Seto, T., & Iizuka, T. (2010). Virtual kyoto project: Digital diorama of the past, present, and future of the historical city of Kyoto *Culture and computing* (pp. 173-187): Springer.

Nir, Y. (1985). The beginings of photography in the Holy Land. *Cathedra, 38*, 67-80.

Röhricht, R. (1890). *Bibliotheca Geographica Palaestinae: Chronologisches Verzeichnis der von 333 bis 1878 Verfassten Literatur über das Heilige Land*. London: John Trotter Publishers.

Rubinowicz, P., & Czyńska, K. (2015). *Study of city landscape heritage using Lidar data and 3D-city models*. Paper presented at the 36th International Symposium on Remote Sensing of Environment Berlin, Germany.

Schaffer, G., Peer, M., & Levin, N. (2016). Quantifying the completeness of and correspondence between two historical maps: a case study from nineteenth-century Palestine. *Cartography and Geographic Information Science, 43*(2), 154-175. doi: 10.1080/15230406.2015.1029519.

Sui, D. (2015). Emerging GIS themes and the six senses of the new mind: is GIS becoming a liberation technology? *Annals of GIS, 21*(1), 1-13. doi: 10.1080/19475683.2014.992958.

Uhl, J. H., Leyk, S., Chiang, Y.-Y., Duan, W., & Knoblock, C. A. (2017). Extracting human settlement footprint from historical topographic map series using context-based machine learning.

Verhagen, J., & Jeneson, C. F. (2012). A Roman Puzzle. Trying to find the Via Belgica with GIS.

Wang, J., Song, J., Chen, M., & Yang, Z. (2015). Road network extraction: A neural-dynamic framework based on deep learning and a finite state machine. *International Journal of Remote Sensing, 36*(12), 3144-3169.

Wang, Y., & Taylor, J. E. (2018). Coupling sentiment and human mobility in natural disasters: a Twitter-based study of the 2014 South Napa Earthquake. *Natural hazards, 92*(2), 907-925.

Wilson, C. W. S. (Cartographer). (1865). Ordnance Survey of Jerusalem; By Captain W. Wilson, R.E. under the direction of Colonel Sir Henry James...1864-5. Engraved at the Ordnance Survey Office, Southampton under the direction of Colonel J. Cameron, R.E.

Zohar, M. (2017). A city hit by an earthquake: an HGIS approach to reconstructing the damage in Tiberias (Israel) in 1837. *International Journal of Geographical Information Science, 31*(1), 81-99. doi: 10.1080/13658816.2016.1188933

Zohar, M. (2019). Follow the road: historical GIS for evaluating the development of routes in the Negev region during the twentieth century. *Cartography and Geographic Information Science, 46*(6), 532-546. doi: 10.1080/15230406.2019.1577176.

APPENDIX

Table 1: RANSAC model results for identifying features appearing in the painting of Henniker. Fields of the table: **S** - feature notation; **Name** – the name of the feature; **H** – the height of the feature above surface; **X, Y, Z** - longitude, latitude and elevation above sea level of the features, respectively; **pXH, pYH** - pixel coordinates of human notation on Henniker's paintings; **rXH, rYH** - pixel coordinates of the RANSAC model on Henniker's painting; **EH** – pixel length difference between human and model notation. The biggest differences of features T, U and of lesser extent G and O are noted in bold; **pXP, pYP** - pixel coordinates of human notation on the photograph; **rXP, rYP** - pixel coordinates of the RANSAC model on the photograph; **EP** – pixel length difference between human and model notation. The biggest differences of features F and R are noted in bold. Summary values of A (average), M (Median), Mi (Min), Mx (Max) and 1Q, 2Q, 3Q (quartiles thresholds) are also listed.

S	Name	H	X	Y	Z	pXH	pYH	rXH	rYH	EH	pXP	pYP	rXP	rYP	EP
A	Al-Nabi Dau'd	12	221795	631010	795	283	213	288	159	54					
B	Wall	10	222186	631291	751	637	341	582	288	76	236	1580	88	1518	16
C	Omar Caliph	15	221987	631380	787	754	227	728	200	38	832	1496	811	1450	51
D	Al-Qalaa'	15	221668	631431	793	832	173	809	203	38	1091	1463	1083	1445	19
E	Al-Aqsa	15	222414	631468	752	857	287	824	311	4	1007	1582	1000	1586	8
F	David citadel	15	221666	631525	796	929	183	896	203	38	1198	1478	1352	1454	**156**
G	Wall	10	222100	631198	753	396	315	473	271	**89**					
H	Al-Faqriah	15	222315	631620	764	1043	239	1064	278	44	1794	1554	1832	1559	38
I	Al-Omar	18	221835	631681	786	1056	198	1050	227	29	1819	1499	1810	1490	13
J	Golden Gate	8	222559	631809	750	1450	363	1455	354	2	3086	1722	3113	1684	47
K	Wall	10	222594	631489	726	858	376	859	425	49	1022	1771	1020	1788	17
L	Harm Al-Sharif	20	222382	631702	768	1158	226	1215	276	76	2201	1520	2252	1573	74
M	Holy Sepulchre	20	221839	631752	792	1105	207	1120	219	19	1978	1500	1996	1491	20
N	Bab Al-Asbat	12	222482	631943	756	1661	307	1585	332	8	3519	1618	3425	1655	12
O	Wall	10	222511	632334	772	2166	389	2124	312	**88**					
P	Al-Malla'wiyah	8	222194	631960	778	1433	261	1437	263	4	2955	1592	2878	1562	82
Q	Custodia T. S.	20	221620	631859	807			1145	195		2053	1423	2047	1471	49
R	Lion's Gate	8	222538	632020	756	1795	379	1742	342	64	4010	1717	3842	1677	**174**
S	Sheich Reichan	10	222189	632065	786	1608	237	1558	249	52					
T	Wall	10	222036	632200	794	1784	255	1589	239	**195**	3154	1528	3198	1547	48
U	Herod's Gate	8	222224	632253	785	1942	321	1755	262	**196**					
V	Santa Anna	12	222495	632081	762	1795	341	1788	324	19					
									A	**56**				**A**	**51**
									M	**44**				**M**	**43**
									Mi	**2**				**Mi**	**8**
									1Q	**19**				**1Q**	**17**
									2Q	**41**				**2Q**	**43**
									3Q	**67**				**3Q**	**57**
									Mx	**196**				**Mx**	**174**